

## Observations of elevated particle number concentration events at a rural site in New England

L. D. Ziemba,<sup>1,2</sup> R. J. Griffin,<sup>1,3</sup> and R. W. Talbot<sup>1</sup>

Received 31 May 2006; revised 6 September 2006; accepted 12 October 2006; published 15 December 2006.

[1] Particle number (PN) concentrations collected over a 4-year period at the Thompson Farm atmospheric observatory in New Hampshire in conjunction with the Atmospheric Investigation, Regional, Modeling, Analysis and Prediction (AIRMAP) program are reported here. One hundred and ninety-five elevated PN events, occurring on approximately 7.5% of sampled days, were identified on the basis of PN concentration statistics. Events were segregated into five event types defined according to auxiliary measurements and event duration. A distinct seasonality is observed, with PN concentrations peaking in the winter and PN event observation most frequent in the spring. Long-lived PN events associated with clean, northwesterly flow and PN events associated with primary pollutant plumes were observed most frequently, each making up 33% of all identified events. PN events characterized by air masses enriched in sulfur dioxide and originating southeast of Thompson Farm contributed 20% of the total PN events. All PN events are well correlated with solar intensity, with estimated particle diameters during events well below 100 nm. No relationship between PN concentrations and temperature or precipitation could be identified on either seasonal or daily timescales. PN events described here are unique and exclusive of other aerosol mass loading events previously identified at Thompson Farm.

**Citation:** Ziemba, L. D., R. J. Griffin, and R. W. Talbot (2006), Observations of elevated particle number concentration events at a rural site in New England, *J. Geophys. Res.*, *111*, D23S34, doi:10.1029/2006JD007607.

### 1. Introduction

[2] The Earth's climate is influenced greatly by the physical and chemical properties exhibited by atmospheric aerosols, which alter cloud properties and the Earth's radiative balance [Charlson *et al.*, 1992]. Particle number (PN) concentrations give insight into aerosol sizes, sources, and formation processes. The smallest aerosols, those with diameters less than 100 nm, lie in the nuclei mode and account for the largest PN concentrations. Aerosols of this size enter the atmosphere by two distinct pathways: direct emission or in situ formation. Combustion processes are the main primary sources of nuclei mode aerosols, while homogeneous nucleation is the main secondary process producing nuclei mode aerosols [Whitby and Sverdrup, 1980].

[3] Homogeneous nucleation events have been observed in many different locations [Kulmala, 2003]. Traditional thinking indicates that remote regions would be favored for homogeneous nucleation events because of very low con-

centrations of preexisting aerosols that can scavenge condensable gases and inhibit nucleation. Homogeneous nucleation has been observed in the tropical free troposphere [Clarke *et al.*, 1999], coastal regions [O'Dowd *et al.*, 2002], the boreal forest [Mäkelä *et al.*, 1997], and the marine boundary layer [Weber *et al.*, 1995]. Homogeneous nucleation, however, has also been observed in more polluted continental regions [Birmili and Wiedensohler, 2000; Harrison *et al.*, 2000; Mozurkewich *et al.*, 2004], urban areas [Alam *et al.*, 2003; Stanier *et al.*, 2004], and in Asian plumes [Weber *et al.*, 2003a]. Homogeneous nucleation therefore is now thought to occur ubiquitously in the troposphere.

[4] Stanier *et al.* [2004] defined a nucleation event as a significant increase in the smallest fraction of nuclei mode (3 nm to 10 nm in diameter) PN concentrations without a concurrent increase in the mixing ratios of nitric oxide (NO) and carbon monoxide (CO), which are associated with primary combustion emissions. Events defined by Stanier *et al.* [2004] were correlated with solar radiation, which promotes photochemistry. Birmili and Wiedensohler [2000] classified aerosol formation events as periods when ultrafine aerosol PN concentrations exceeded  $10,000 \text{ cm}^{-3}$  for over 4 hours. Alam *et al.* [2003] also included a lack of concurrent increases in the mixing ratios of sulfur dioxide (SO<sub>2</sub>) and nitrogen oxides (NO<sub>x</sub>) in their description of homogeneous nucleation criteria.

[5] The seasonality of events associated with increased PN concentrations is not well characterized, especially on a

<sup>1</sup>Institute for the Study of Earth, Oceans, and Space, Climate Change Research Center, University of New Hampshire, Durham, New Hampshire, USA.

<sup>2</sup>Formerly at Department of Earth Sciences, University of New Hampshire, Durham, New Hampshire, USA.

<sup>3</sup>Also at Department of Earth Sciences, University of New Hampshire, Durham, New Hampshire, USA.

**Table 1.** Auxiliary Measurements for Analysis of Particle Number (PN) Concentrations

Measurement	Method	Instrument	Reference
Carbon monoxide (CO)	infrared spectroscopy at 4600 nm	Thermo Environmental Instruments <sup>a</sup> (TEI) 48CTL	<i>Mao and Talbot</i> [2004]
Nitric oxide (NO) and total reactive nitrogen (NO <sub>x</sub> )	chemiluminescence	TEI <sup>a</sup> 42C	<i>Mao and Talbot</i> [2004]
Ozone (O <sub>3</sub> )	ultraviolet spectroscopy at 254 nm	TEI <sup>1</sup> 49C-PS	<i>Mao and Talbot</i> [2004]
NO <sub>2</sub> photolysis rate constant ( $j_{\text{NO}_2}$ )	filter radiometry	Radiometer <sup>b</sup>	<i>Shetter et al.</i> [2003]
Aerosol optical absorption	absorption photometry	particle/soot absorption photometer (PSAP) <sup>c</sup>	<i>Bond et al.</i> [1999]
Aerosol mass loadings	filter collection and ion chromatographic (IC) analysis	Fluropore™ filters <sup>d</sup> , Dionex <sup>e</sup> IC columns	<i>DeBell et al.</i> [2004a]
Black carbon (BC)	light attenuation at 880 nm	aethalometer <sup>c</sup>	<i>Parungo et al.</i> [1994]
Aerosol-scattering coefficient	transmittance of light at 550 nm	nephelometer <sup>f</sup>	<i>Day and Malm</i> [2001]
Meteorological data (wind direction, wind speed, temperature, relative humidity)	various techniques	platinum resistance thermometer and Met One model 014A anemometer	<i>Vose</i> [2005]
Precipitation	rain gauge	Geonor model T-200B <sup>g</sup>	<i>Vose</i> [2005]

<sup>a</sup>Franklin, Massachusetts, United States.

<sup>b</sup>Metcon, Inc., Boulder, Colorado, United States.

<sup>c</sup>Radiance Research, Seattle, Washington, United States.

<sup>d</sup>Millipore, Bedford, Massachusetts, United States.

<sup>e</sup>Sunnyvale, California, United States.

<sup>f</sup>Magee Scientific Company, Berkeley, California, United States.

<sup>g</sup>Milford, Pennsylvania, United States.

regional basis. Here, we present observations of enhanced PN concentration events from a rural site in northern New England over a 4-year period. Our discussion highlights a unique seasonality and identifies potential sources of PN events as a function of chemical and meteorological characteristics. A comparison of this data set to other long-term studies is included, as *Vehkamaki et al.* [2004] reported a unique 5-year record of aerosol growth events at a remote Arctic site in Varrio, Finland, and *Birmili et al.* [2003] have observed similar events over a 2.5-year period from a mountaintop site in southern Germany. Comparisons to sampling campaigns of shorter duration are also made.

## 2. Site Description and Instrumentation

[6] Sampling was performed at the University of New Hampshire (UNH) Atmospheric Observing Station at Thompson Farm (TF) in conjunction with the Atmospheric Investigation, Regional, Modeling, Analysis and Prediction (AIRMAP) program ([www.airmap.unh.edu](http://www.airmap.unh.edu)). This site is located 24 m above sea level in Durham, NH, at 43.11°N, 70.95°W. TF is unique because it is a rural site influenced by regional features such as the Atlantic Ocean, urban centers of the Atlantic seaboard, industrial activity in the midwestern United States and the Ohio River valley, and pristine areas at high latitudes in Canada.

[7] PN concentrations were measured continuously at 15 m above the ground using a condensation particle counter (CPC 3022A, TSI Inc., St. Paul, Minnesota, United States) that counts individual aerosol particles with a size range of 7 nm to 3 μm with an efficiency of 50% between 7 nm and 15 nm and greater than 90% above 15 nm. This instrument operates at a flow rate of 0.3 L min<sup>-1</sup>, uses butanol as a condensing liquid, and counts aerosol particles

up to concentrations of 1 × 10<sup>7</sup> cm<sup>-3</sup> by standard optical methods. Data were saved and analyzed as 1-min averages. Measurements of several other compounds were used to characterize the PN events, and details of these measurements are summarized in Table 1.

## 3. Methods

[8] PN events were identified on the basis of the magnitude and duration of enhanced PN concentrations on a daily basis. A PN event threshold was defined as the median PN concentration for the entire 4-year data set plus twice the standard deviation (SD). The median PN concentration of 6,600 cm<sup>-3</sup> ± 6,000 (SD) cm<sup>-3</sup> resulted in a PN event threshold of 18,600 cm<sup>-3</sup> for this study. Days in which PN concentrations exceeded this threshold for greater than 2 hours were then classified as event days. Likewise, days in which PN concentrations did not exceed the PN threshold for greater than 2 hours were classified as nonevent days. PN concentration events lasting less than 2 hours were disregarded to remove very short lived, large magnitude PN concentrations thought to be influenced by a local source. The 5th percentile PN concentration has been used to define an estimated PN background concentration, which is used to assess the potential influence of seasonal variability in background PN concentrations on event definition.

[9] Days exhibiting events were segregated into event types on the basis of the temporal length of the event and whether or not the event coincided with increases in SO<sub>2</sub> or other primary pollutants. Sulfur dioxide is segregated from other primary pollutants because of its potential as a precursor to nucleating species [*Verheggen and Mozurkewich*, 2002]. The five event types are summarized in Figure 1 and are described in more detail here. Event

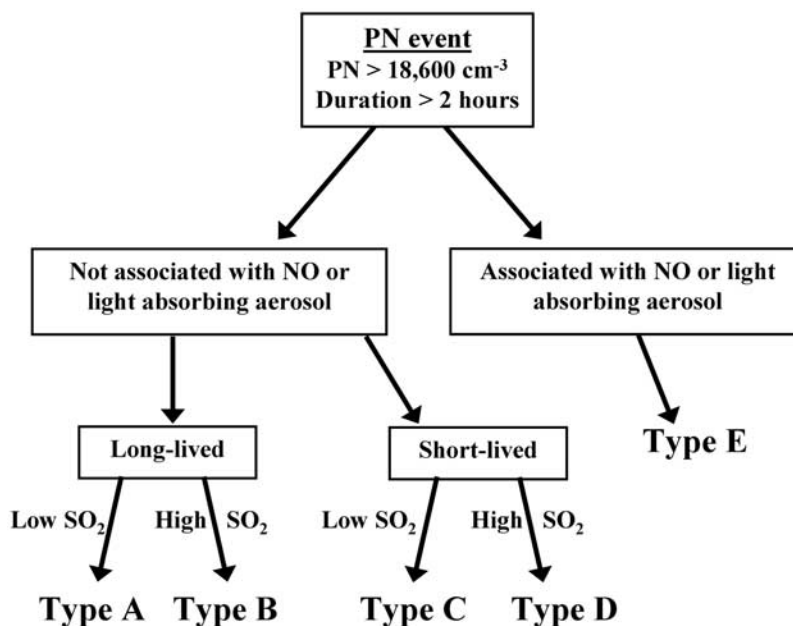


**Figure 1.** Particle number (PN) event-type segregation. Long-lived events have a duration of greater than 5 hours; short-lived events have a duration of less than 5 hours.

duration was calculated by visual inspection, on the basis of the time of the initial increase in PN concentration and the time PN concentration returned to the initial PN or when PN concentration ceased to decrease. A second threshold of 5 hours was used to separate long-lived and short-lived events on the basis of previous observations of the duration of nucleation events [Birmili and Wiedensohler, 2000; Vehkamäki et al., 2004]. Events with duration greater than this threshold of 5 hours (types A and B) represented more regional-scale events and were isolated from localized events of shorter duration than the 5-hour threshold (types C and D). These shorter events (between 2 and 5 hours in duration) may or may not be less regional in scope but certainly represent different conditions. Events considered to be coincident with increased  $\text{SO}_2$  (types B and D) exhibited daytime (1500–2100 UT) average concentrations exceeding the 4-year daytime average  $\text{SO}_2$  mixing ratio of 1.68 parts per billion (ppb) and are referred to as “high- $\text{SO}_2$ ” events. Conversely, type A and C events are associated with daytime average  $\text{SO}_2$  concentrations below 1.68 ppb and are referred to as “low  $\text{SO}_2$ ” events. Daytime average  $\text{SO}_2$  concentrations were used because all PN events were observed during these hours. Sulfur dioxide concentrations were selected as event criteria on the basis of previous theory and observations, which suggest binary and ternary homogeneous nucleation mechanisms involving sulfuric acid as the dominant nucleation mechanism [Korhonen et al., 1999; Birmili and Wiedensohler, 2000]. This criterion is contrary to the observations of Alam et al. [2003], who identified particle formation events in an urban environment and excluded periods of increased  $\text{SO}_2$  to avoid influence from combustion sources. For this analysis, any observed increases in  $\text{SO}_2$  concentration during the PN concentration increase, not necessarily directly correlated with the PN increase, were used for classification purposes.

[10] PN events of type E are associated with enhanced aerosol absorption coefficients or enhanced NO concentrations above the 4-year daytime averages of  $3.44 \text{ Mm}^{-1}$  and 0.83 ppb, respectively. Nitric oxide and absorbing aerosol were selected on the basis of association with primary pollution plumes and combustion [Lowenthal et al., 1994; Lee et al., 1997]. Type E events were identified independent of event duration (but were still greater than 2 hours in duration) and  $\text{SO}_2$  enhancement and were used here to segregate events potentially associated with primary combustion emissions.

## 4. Results

### 4.1. Seasonal Trends in PN Concentration and PN Events

[11] The full time series of PN concentrations at 1-hour resolution for 1 December 2001 through 30 September 2005 is presented in Figure 2. Fifth, 50th, and 95th percentile statistics sorted by season and year are reported in Tables 2a and 2b. PN concentrations ranged from  $411 \text{ cm}^{-3}$  to  $260,000 \text{ cm}^{-3}$  (off the scale of Figure 2) with an average PN concentration of  $7,735 \text{ cm}^{-3}$  and a median PN concentration of  $6,600 \text{ cm}^{-3}$ . The background PN concentration (the 5th percentile value calculated every 30 days) is also presented in Figure 2 and had an average of  $2,210 \text{ cm}^{-3}$  for the 4-year data set, approximately 3 times lower than the median concentration. Little variability in background PN concentration is observed between seasons. Variability in PN concentrations is evident and indicates clearly the influence of differing meteorology, emissions, and air mass chemistry.

[12] The 1-min PN data averaged to 1 hour have been analyzed for seasonal trends. Average monthly and median monthly values are reported in Figure 3. Both average and median values have minima in August and maxima in

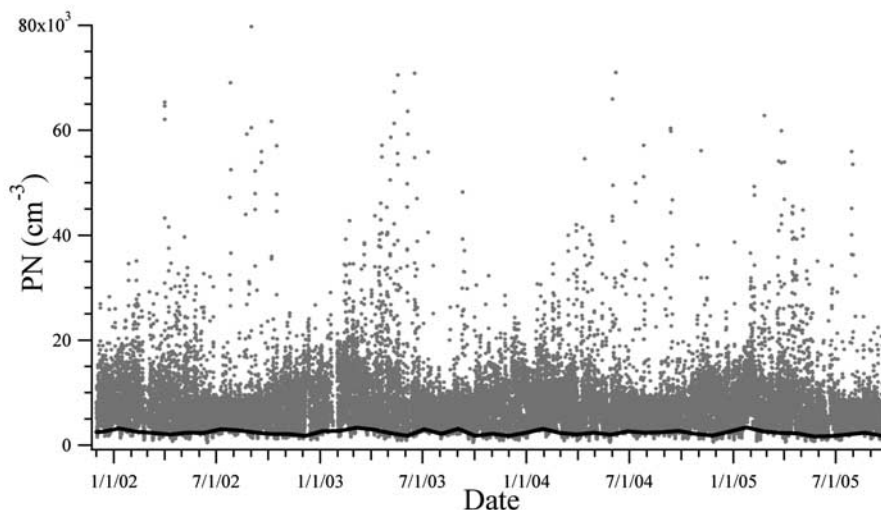


**Figure 2.** Time series for PN from 1 December 2001 through 30 September 2005 using 1-hour averaged data. The black line represents the background PN concentration.

February; average and median PN concentrations are 61 and 59% greater in February compared to August. This seasonal distribution is likely due to 3 factors: (1) decreased boundary layer height associated with less daytime heating at the surface during the winter; (2) increased photochemical reaction rates and thus increased overall aerosol mass loading in the summer; and (3) increased depositional particle loss due to increased atmospheric turbulence during the summer. Ninety-fifth percentile sulfate ( $\text{SO}_4^{2-}$ ) aerosol mass loadings at TF are 122% and 95% higher in the summer than in winter or spring respectively (L. D. Ziemba et al., Aerosol acidity in rural New England: Temporal trends and source region analysis, submitted to *Journal of Geophysical Research*, 2006). Such increased preexisting aerosol mass has been shown to inhibit particle nucleation and thus inhibit large PN concentrations [Alam et al., 2003]. While average values are consistently greater than median values throughout the year, this difference (also shown in Figure 3 as the ratio of the average to the median) is largest during the spring (a difference of  $1800 \text{ cm}^{-3}$  in April and May) and smallest during the summer and fall (differences of  $600 \text{ cm}^{-3}$  in August and  $400 \text{ cm}^{-3}$  in November). This indicates that high-magnitude PN events occurred during the spring and strongly influenced the average PN concentration.

[13] The seasonality of enhanced PN events has also been analyzed. Overall, PN events occur most frequently during

the winter (55 events total,  $0.15 \text{ events d}^{-1}$ , one event approximately every 7 days) and spring (89 events,  $0.24 \text{ events d}^{-1}$ , one event approximately every 4 days) and much less frequently during the summer (28 events,  $0.08 \text{ events d}^{-1}$ , one event approximately every thirteen days) and fall (23 events,  $0.08 \text{ events d}^{-1}$ , one event approximately every thirteen days). The highest PN frequency was observed in April ( $0.33 \text{ events d}^{-1}$ , one event approximately every 3 days) and the lowest observed PN frequency was observed during August ( $0.03 \text{ events d}^{-1}$ , less than one event every month). For comparison, Vehkamäki et al. [2004] report a seasonal formation event maximum during the spring with a slightly less frequent event occurrence ( $0.2 \text{ events d}^{-1}$ ).

#### 4.2. Type A Events: Long-Lived and Low $\text{SO}_2$

[14] Over the full sampling period, type A events were observed 64 times and account for 33% of all PN events. These events were observed almost exclusively during the months of February through May (78% of all type A events were observed during this period) and none were observed from July through September (Figure 4a). On a year-to-year basis, the type A seasonal distribution is consistent: 19 events in 2002, 15 events in 2003, 16 events in 2004, and 14 events in 2005. Diurnal box plots for type A events are presented in Figure 5a, along with the diurnal trend for 95th percentile and 5th percentile  $j_{\text{NO}_2}$  measurements and

**Table 2a.** Statistics for PN Concentrations and Event Occurrence Sorted by Season and Year<sup>a</sup>

	Winter					Spring				
	2002	2003	2004	2005	All	2002	2003	2004	2005	All
5th	2690	2280	2500	2430	2470	2160	2310	1870	2110	2090
50th	7660	8420	7560	7930	7860	6570	7520	6730	6710	6880
95th	17,500	19,700	18,400	17,200	18,300	18,400	22,500	16,600	19,200	19,400
Events	13	13	16	13	55	19	29	14	27	89

<sup>a</sup>All refers to statistics for the full data set (all years) for each season and the total number of events for each season. Events refers to the total number of events during each year. Seasons are defined as follows: Winter = December, January, and February; spring = March, April, and May; summer = June, July, and August; fall = September, October, and November. January defines the winter year.

**Table 2b.** Statistics for PN Concentrations and Event Occurrence Sorted by Season and Year<sup>a</sup>

	Summer					Fall				
	2002	2003	2004	2005	All	2002	2003	2004	2005	All
5th	2520	2310	2470	1900	2290	2120	1930	2130	–	2,070
50th	5750	5720	5720	5490	5670	6700	6270	6790	–	6,570
95th	11,100	12,600	11,300	10,800	11,500	14,400	14,500	14,300	–	14,400
Events	10	8	8	2	28	7	8	8	–	23

<sup>a</sup>As for Table 2a.

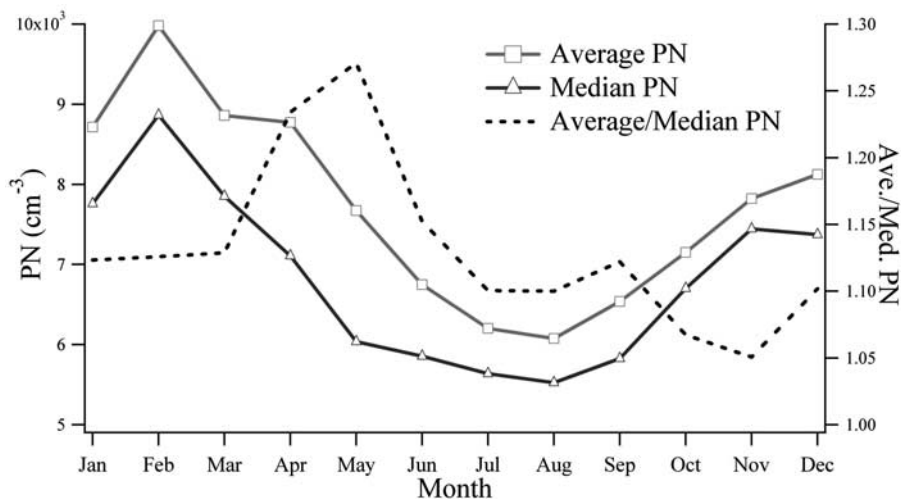
average SO<sub>2</sub> mixing ratios during events. All events of this type occur during daylight hours. PN concentrations increase following sunrise, at approximately 1000–1200 UT, peak slightly before maximum j<sub>NO2</sub> (1500–1700 UT), and decrease gradually in the afternoon. Average SO<sub>2</sub> concentrations show a similar early morning increase at 1200 UT but decreased during times of maximum j<sub>NO2</sub> and PN. The small range in j<sub>NO2</sub> (illustrated by 5th and 95th percentile j<sub>NO2</sub> in Figure 5a) and smoothness of the PN concentration curve indicate that events of this type probably occur during clear days with few interruptions in solar radiation, making in-cloud aerosol production less likely.

[15] The potential source regions for PN events were investigated using wind direction profiles, presented in Figure 6. Here, the radial axes are in units of % of occurrence and each wind rose is shaded by the magnitude of PN concentration. Samples with wind speeds less than 1 m s<sup>-1</sup> were ignored to avoid erroneous wind direction data due to meandering [Anfossi *et al.*, 2005]. For comparison, samples from nonevent days are plotted in a similar manner and presented in Figure 6f. Northwestern winds are dominant during type A events (Figure 6a), indicating that high-latitude locations in Canada are potential source regions. Backward trajectories were computed using the HYSPLIT Lagrangian transport model (R. R. Draxler and G. D. Rolph, HYSPLIT (Hybrid Single-Aerosol Lagrangian Integrated Trajectory) Model access via NOAA ARL READY Website, 2003, available at <http://www.arl.noaa.gov/ready/hysplit4.html>) to confirm source regions of several events during northwesterly surface flow. All backward trajectories were initialized at 500 m above ground level at 1300 local time and

were run for 48 hours. During five events, average surface wind directions between 270° and 360° were associated with backward trajectories passing over northern New Hampshire or northern Vermont and originating in northern Canada. Daytime concentrations significantly below average for NO, NO<sub>3</sub>, SO<sub>2</sub>, and BC (83, 67, 70, and 65%, respectively) were observed during type A events, consistent with typically less polluted air masses from this region. Statistics for auxiliary measurements are presented in Table 3 for all PN event types. Decreased RH (49% less than average, from Table 3) is also consistent with air masses originating from the colder, Canadian region. The source region for type A events is unique compared to all other event types and is distinct from days on which no events were observed, as shown in Figure 6f.

#### 4.3. Type B and Type D: High SO<sub>2</sub>

[16] PN events associated with high SO<sub>2</sub> concentrations (types B and D) occurred less frequently than did type A PN events, accounting for 20% of the total number of observed events. Daytime SO<sub>2</sub> concentrations during these events were 73 and 79% greater than average SO<sub>2</sub> concentrations. Diurnal SO<sub>2</sub> profiles for both event types illustrate the elevated concentrations (Figures 5b and 5d), and SO<sub>2</sub> concentrations are especially well correlated with PN concentrations for type D events. These events are characterized by similar source regions (Figures 6b and 6d) and air mass chemistry (Table 3) and all occur during daylight hours (Figures 5b and 5d). The range in diurnal j<sub>NO2</sub> values (indicated by the difference between 5th and 95th percentile

**Figure 3.** Monthly average PN and median PN concentrations from 1-hour averaged data.

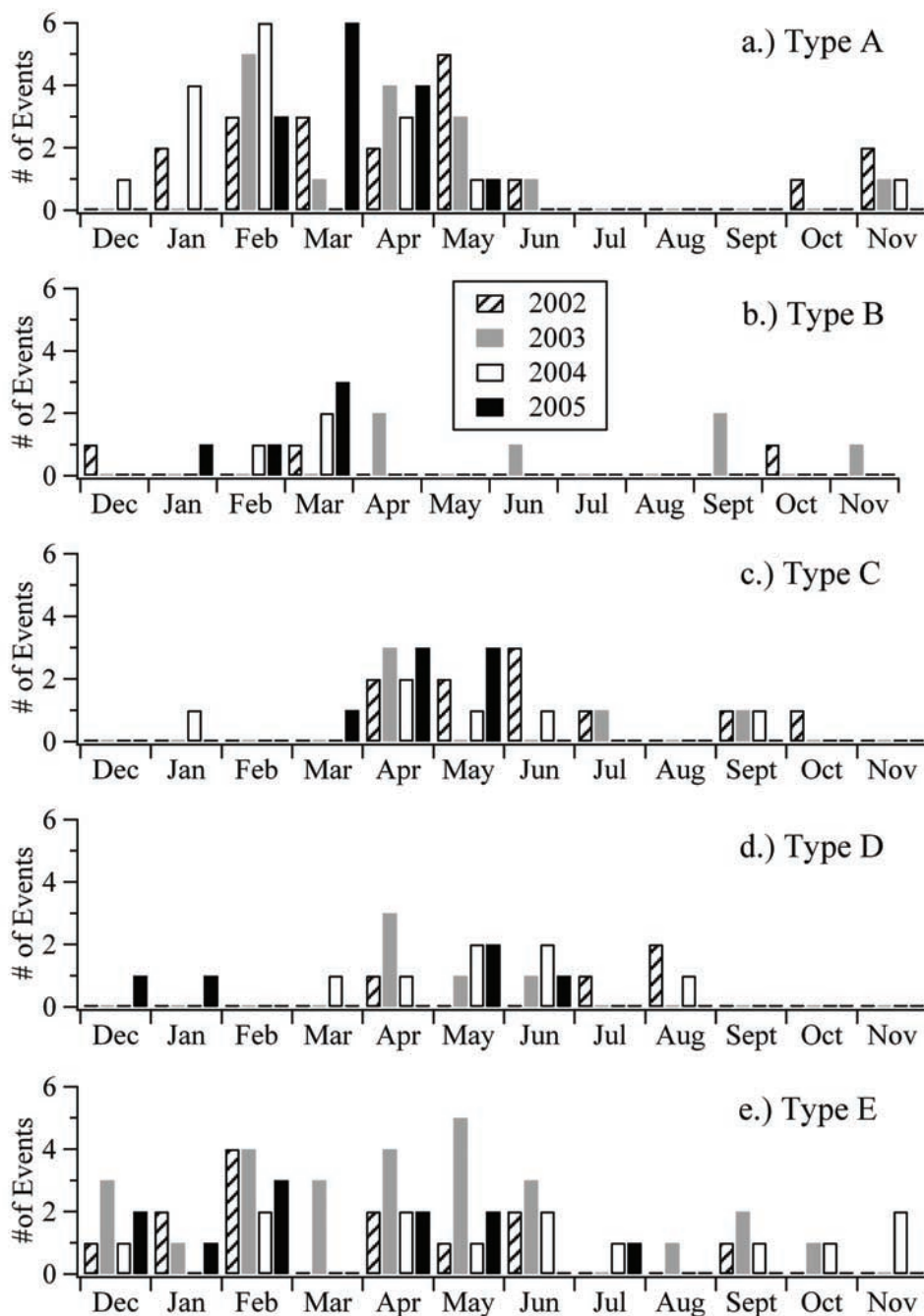


**Figure 4.** Monthly frequency of event occurrence sorted by year: (a) type A; (b) type B; (c) type C; (d) type D; (e) type E.

values) for long-lasting high-SO<sub>2</sub> events, shown in Figure 5b, is similar to that of type A and indicates clear sky conditions. A larger  $j_{\text{NO}_2}$  range (56%, compared to 37% for type B) observed during short-lived high-SO<sub>2</sub> events (Figure 5d) probably indicates intermittent cloud cover during events and would increase the likelihood of in-cloud processing. Unique to high-SO<sub>2</sub> events is a significantly larger PN magnitude. Ninety-fifth percentile PN concentrations were 40,300 and 39,900 cm<sup>-3</sup> for types B and D, compared to 30,500 and 28,400 for the low-SO<sub>2</sub> events of type A and C.

[17] Type B events had a monthly distribution similar to that of type A events; 59% occurred during February through April (Figure 4b). Type D events had a distribution similar to that of type C events, as discussed below; 86% of type D events occurred from April through August. This shift in seasonal distribution likely indicates a difference in chemical formation pathway or cloud conditions. Source regions for both types B and D are primarily from the southeastern wind direction, where air masses passing over urban centers would be more likely to have enhanced SO<sub>2</sub>. While surface winds were consistently from the southeast,

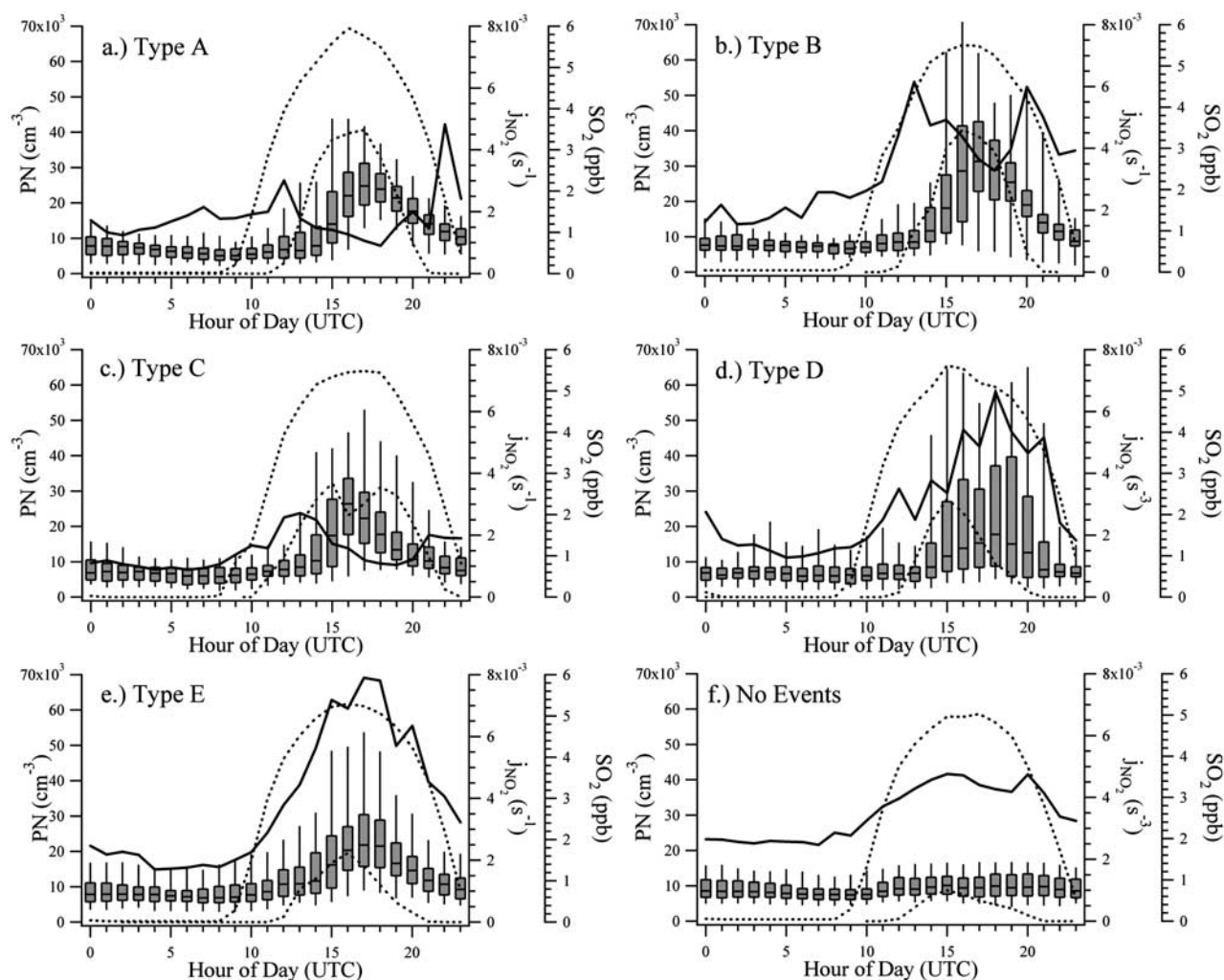


**Figure 5.** Diurnal box plots for events: (a) type A; (b) type B; (c) type C; (d) type D; (e) type E; (f) nonevent days. Lines inside each box represent the median value. Top and bottom of each box represent the 75th and 25th percentiles, respectively. Top and bottom of each whisker represent the 95th and 5th percentiles, respectively. Hour of the day is in UTC which equals local time plus 5 hours (EST) and local time plus 4 hours (EDT). (dotted lines) Fifth and 95th percentile  $j_{\text{NO}_2}$  values for each event type; (solid line) average hourly  $\text{SO}_2$  concentrations.

backward trajectories were more variable. Air masses arriving from the southeast either passed over Boston, MA, and the eastern seaboard or followed the coast of Maine. The average  $\text{NO}/\text{NO}_y$  ratio for type B and D events was similar to type A events (0.12, 0.11, and 0.12, respectively), indicating comparable photochemical age, although the presence of  $\text{SO}_2$  in highly processed air masses could indicate a more local source or mixing of two different air mass types. The combined number of type B and D events is consistent from year-to-year as 7 were observed in 2002, 11 in 2003, 10 in 2004, and 10 in 2005.

#### 4.4. Type C Events: Short-Lived, Low $\text{SO}_2$

[18] Type C events were observed less frequently than either type A events or high- $\text{SO}_2$  events (types B and D), accounting for only 15% of the observed total. Associated measurements indicate that these events are most likely a mix of the previously discussed event types (types A, B, and D). Average daytime  $\text{SO}_2$  concentrations were 53% lower

than the average, shown in Table 3. From Figure 6c, source regions are likely similar to both high- $\text{SO}_2$  event types, given consistent southeastern winds, although the variability in backward trajectories was similar to the high- $\text{SO}_2$  events. The seasonal distributions for both short-lived event types (C and D) peak in the summer and spring (Figures 4c and 4d) and occur very infrequently in the fall and winter. The diurnal  $j_{\text{NO}_2}$  profile for type C events indicates periods of interrupted solar radiation similar to type D events (Figure 5c) and a morning increase and midday minimum of  $\text{SO}_2$  concentrations, similar to the diurnal  $\text{SO}_2$  trend observed during type A events.

#### 4.5. Type E Events: Primary Emissions

[19] PN concentration events likely associated with primary emissions occurred at this site as frequently as type A events (making up 33% of all events) and were characterized by higher  $\text{CO}$ ,  $\text{NO}$ ,  $\text{NO}_y$ , and  $\text{BC}$  concentrations relative to all other event types (Table 3). Daytime concen-

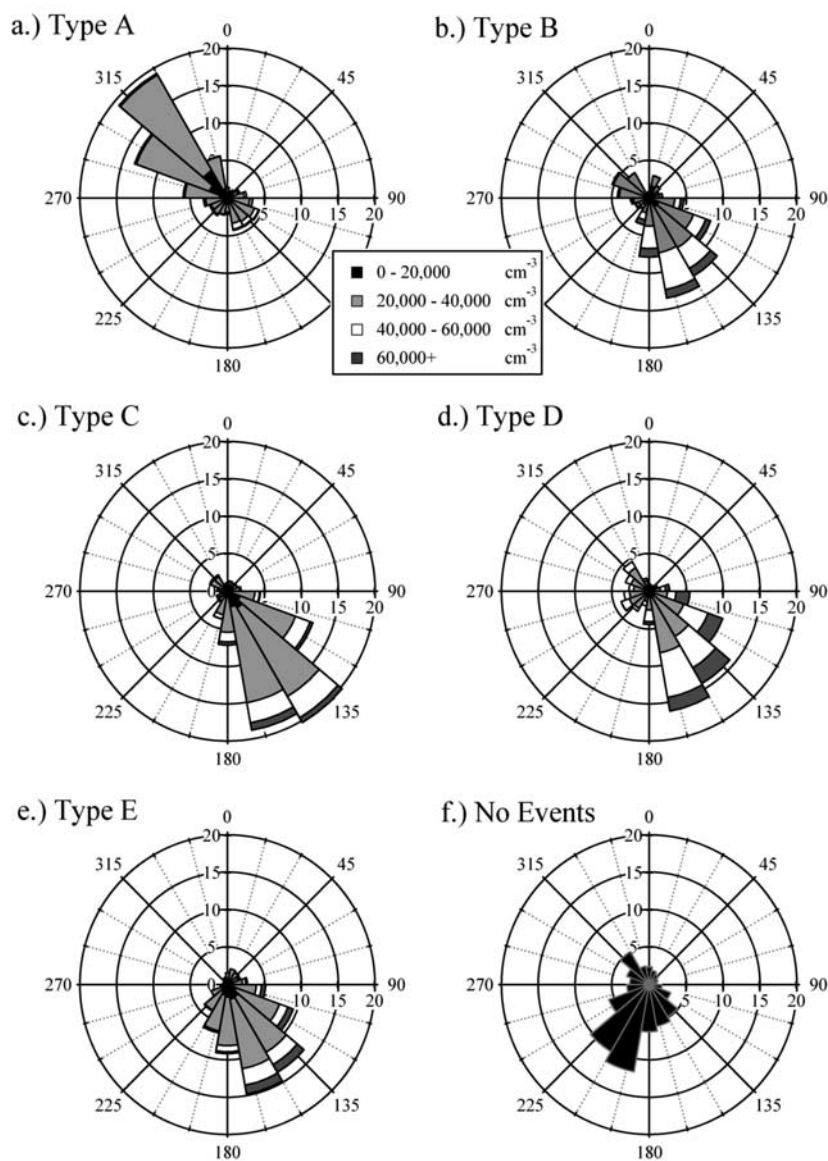


**Figure 6.** Wind direction distributions for events. (a) type A; (b) type B; (c) type C; (d) type D; (e) type E; (f) nonevent days. Radial axis is in units of % occurrence. Due north is represented by  $0^\circ$ .

**Table 3.** Statistics for Event Types<sup>a</sup>

	A	B	C	D	E	All Data
Number of events	64	17	29	21	64	195
CO	170	183	161	156	207	188
$j_{\text{NO}_2}$	0.0057	0.0055	0.0056	0.0047	0.0045	0.0038
RH	30.4	38.5	42.0	47.2	50.5	59.8
Wind speed	3.37	2.47	3.00	2.25	2.26	1.45
NO	0.24	0.48	0.29	0.32	2.51	1.39
$\text{NO}_y$	1.98	4.04	2.85	2.79	10.8	6.09
$\text{O}_3$	42.6	42.9	44.1	39.9	35.9	34.8
$\text{SO}_2$	0.64	3.64	0.99	3.77	5.26	2.11
Duration	6.8	6.2	3.1	3.2	4.1	NA
BC	118	175	173	165	317	338
Absorption coefficient	1.35	1.72	1.92	1.96	3.49	3.44
Scattering coefficient	9.45	12.5	10.5	16.2	19.0	26.2

<sup>a</sup>Units in parentheses as follows: CO (ppb),  $j_{\text{NO}_2}$  ( $\text{s}^{-1}$ ), RH (%), NO (ppb),  $\text{NO}_y$  (ppb),  $\text{O}_3$  (ppb),  $\text{SO}_2$  (ppb), duration (hours), BC ( $\text{ng m}^{-3}$ ), absorption coefficient ( $\text{Mm}^{-1}$ ), and scattering coefficient ( $\text{Mm}^{-1}$ ). Values for events are daytime averages, where daytime is defined as 1500 UT through 2100 UT. All Data refers to statistics for the full data set. NA denotes statistics that are not applicable.

trations of NO during type E events were 90% greater than during type A events and 45% greater than the data set average. A higher NO/NO<sub>y</sub> ratio (0.23) compared to other event types (0.12 for type A) is consistent with less photochemical aging. Type E events were characterized by a large range in J<sub>NO2</sub>, a midday peak in PN and well correlated peak in SO<sub>2</sub> concentration, and mainly south-eastern source regions, as shown in Figures 5e and 6e. Type E events were observed in every month of the year, although infrequently from July through November (Figure 4e). The year 2003 was unique in terms of type E event occurrence; 27 were observed during this year compared to 13 in 2002, 13 in 2004, and 11 in 2005. Driving this anomaly was spring 2003, when 55% of all spring type E events were recorded.

## 5. Discussion

### 5.1. Temperature, Precipitation, and Climate Influence

[20] This 4-year data set allows the opportunity to explore the influence of climate on seasonal PN concentrations. Data from the Northeast Regional Climate Center were used to determine if any correlations between temperature/precipitation anomalies and elevated PN concentrations exist. Wet deposition is a major loss mechanism of aerosol, while temperature greatly affects aerosol formation and growth through photochemical reaction rates and the vapor pressure of aerosol constituents. “Normal” temperature and precipitation values were defined as the average for each season from 1971–2000. No correlations between seasons of high and low PN concentration and temperature were observed. To highlight this conclusion, extreme seasons are presented here. The highest PN concentrations (and the highest number of events) were observed during spring 2003 (Table 2a), a season that was only slightly below average in terms of temperature (1.9°C below normal) and total precipitation (12.7 mm below normal). In contrast, no statistical deviation from PN concentration average (and total PN events) was observed in winter 2002 (Table 2a), which was the warmest winter on record in the state of New Hampshire since 1895 (6.7°C above average). The year 2005 had the fourth highest spring precipitation measured in New Hampshire since 1895 (101.6 mm greater than normal), and no extreme PN concentrations were measured, as the observed 95th percentile PN concentration was only 1% lower than average for the entire spring data set.

[21] The potential for correlations between PN event observation and rain or temperature anomalies was also analyzed on smaller, day-to-day timescales. Rain events produce conditions favorable for observation of high PN concentrations by washing out preexisting aerosols that act as condensational sinks. No correlation between rainfall events and PN events of any type was observed, regardless of the timing of the rain event (the rain event occurring within the 24 hours previous to the PN event). PN concentrations were generally low during precipitation, and few events were observed directly following rain. Possible temperature dependence on PN events was also investigated on a shorter timescale by comparing the daytime temperature during events with both the average daytime temperature for the previous day and the average daytime

temperature for the 14 previous days. No temperature correlation could be made, indicating that very few PN events were preceded by large temperature changes and that temperatures during PN events were seldom extreme compared to the preceding 2-week average.

### 5.2. Previously Identified Aerosol Events at TF

[22] Previously documented regional high aerosol mass loading events that occurred in the northeastern United States during this study period were examined to see if they fit the criteria for classification as PN events. *DeBell et al.* [2004b] identified a 2-day period, 7–8 July 2002, when the northeastern United States was influenced by a large smoke plume originating from Quebec, Canada. This plume was characterized by extremely elevated CO concentrations (which peaked at 758 ppb, > 99th percentile at TF), aerosol-scattering coefficients (which peaked at 405 Mm<sup>-1</sup>, > 99th percentile at TF), and 24-hour average PM<sub>2.5</sub> mass (which peaked at 338 μg m<sup>-3</sup>, the highest value observed at TF). No PN event was identified during this period, as PN concentrations did not exceed 8,000 cm<sup>-3</sup> during the event. The calculated average aerosol diameter (using the method described in section 5.4) during the smoke event was approximately 448 nm, consistent with transported aerosol [*Marquez et al.*, 2005].

[23] *Fischer and Talbot* [2005] identified three unique regional events when aerosol nitrate (NO<sub>3</sub><sup>-</sup>) molar concentrations met or exceeded aerosol SO<sub>4</sub><sup>2-</sup> molar concentrations from 24-hour bulk filter analysis; two of these NO<sub>3</sub><sup>-</sup> events occurred during this study period. These events were observed during the winter and were attributed to excess ammonia due to severe warming in the midwestern United States. Neither of the documented NO<sub>3</sub><sup>-</sup> events was classified as PN events, consistent with increased preexisting aerosol concentrations that inhibit new particle formation.

### 5.3. Regional Comparison

[24] To put these results into context, PN concentrations observed from this study are compared to instances of particle nucleation in other regions. Although our analysis does not identify nucleation events explicitly, the PN events documented here are likely the result of particle growth following nucleation. Therefore comparison to previous nucleation literature is useful.

[25] *Stanier et al.* [2004] report an average peak PN concentration of approximately 45,000 cm<sup>-3</sup> during observed nucleation events for particles of 3–500 nm in diameter at a site in Pittsburgh, PA during the Pittsburgh Air Quality Study from July 2001 through June 2002. A small, coal-fired heating plant is located a short distance (0.8 km) from the sampling site. In the study presented here, the average PN concentration during events was approximately 22,000 cm<sup>-3</sup> and is somewhat lower, a discrepancy that is explained by a more rural sampling region, potential differences in particle formation and growth mechanisms, and transport/dilution times. PN concentrations during nucleation events reported by *Komppula et al.* [2003] were considerably lower (2,000 to 4,000 cm<sup>-3</sup>) than those reported here and are likely explained by a much cleaner, Arctic measurement site. Median PN concentrations in urban Toronto, Canada (submicron diameter) measured over 1 full year were approximately 3 times those measured at TF [*Jeong et*

*al.*, 2006] and only slightly higher at an urban Rochester, NY site (sub-470 nm), differences likely due to instrument detection limits and influence of local primary emissions.

[26] The seasonal pattern exhibited by PN concentration events at the semirural TF site is interesting compared to the seasonality reported from other long data sets regarding PN concentration events. Data reported from the SMEAR I station in northern Finland taken over a 4-year sampling period indicate the majority of nucleation events in that region occur during the spring and summer seasons [Vehkamäki *et al.*, 2004] and were attributable to the spring bloom and increased biogenic activity. Similarly, maximum PN concentrations and observations of particle formation were recorded during summer months during a 2-year study at two sites in northern Finland by Komppula *et al.* [2003]. Jeong *et al.* [2006] documented a similar springtime maximum in regional nucleation events in Rochester, NY, but also observed a large percentage of such events in the fall season. The data from our study show a dissimilar seasonality. Although particle nucleation has not yet been observed at TF definitively, the difference in seasonality of PN events at TF indicates varied nucleation, growth, and transport processes in this area.

#### 5.4. Estimation of Particle Size During Events

[27] A hypothetical upper limit of aerosol diameter during events at TF was estimated by

$$D_p = \left( \frac{6M}{N\rho\pi} \right)^{\frac{1}{3}} \quad (1)$$

where  $D_p$  is particle diameter (m),  $M$  is the average aerosol mass concentration ( $\mu\text{g m}^{-3}$ ),  $N$  is PN concentration ( $\text{m}^{-3}$ ), and  $\rho$  is particle density ( $\mu\text{g m}^{-3}$ ). All aerosol particles are assumed to be spherical and have a density of  $1.2 \text{ g cm}^{-3}$ . An aerosol mass of  $1.7 \mu\text{g m}^{-3}$  is used on the basis of the average  $\text{SO}_4^{2-}$  mass collected on 24-hour bulk aerosol filters during PN events. Aerosol number concentration is estimated from the 95th percentile PN concentration of  $30,100 \text{ cm}^{-3}$  during Type A events. Type A events are considered because of their high observed frequency. A conservative estimate of particle size during these events using equation (1) yields an aerosol diameter of 43 nm. Sulfate mass is used in this calculation, not to imply the chemical composition of the newly formed aerosol, but simply as a reference mass concentration. Mass loadings including organic aerosol would be more appropriate but are not available. It is important to note that if only a fraction of the measured aerosol mass is truly associated with the PN event that the true aerosol diameter during the events are likely to be smaller than the calculated values. This analysis shows the potential for aerosol diameters well below 100 nm, indicating that aerosols associated with these events have not grown significantly and probably are not associated with long-range transport. Aerosols associated with transport events normally lie in the accumulation size mode between 300 and 500 nm [Marquez *et al.*, 2005].

#### 5.5. Nucleation and Growth of Recently Formed Particles

[28] Additional measurements would be necessary to observe particle nucleation and to determine the exact formation

pathways and associated chemical composition of newly formed particles. Particle size distributions are extremely useful for identifying nucleation events [Komppula *et al.*, 2003; Vehkamäki *et al.*, 2004]. Because the current instrumentation lacks detection below seven nanometers, the PN events presented here are likely observations of the growth of recently formed particles, either at TF or somewhere upwind. A range of growth rates between 1 and  $20 \text{ nm h}^{-1}$  have been measured in different environments [Komppula *et al.*, 2003; Mozurkewich *et al.*, 2004; Stolzenburg *et al.*, 2005], indicating that some growth time following nucleation would be necessary before particles are detected by the CPC used in this study. Meteorological and associated gas-phase measurements allow some inferences into the potential formation and growth mechanisms during these events, but more conclusive findings would require more detailed measurement of nucleation mode aerosol. Given the  $\text{SO}_2$  levels presented in Figure 5, nucleation involving sulfuric acid cannot be excluded definitively for any of the event types. The discussion below aims only to highlight other potential particle formation and growth mechanisms on the basis of pollutant levels and wind direction.

[29] Particle growth during type A events potentially involves organic biogenic precursors, given low concentrations of  $\text{SO}_2$  (70% lower than the average of all data), northwestern source regions, and late winter/early spring seasonality. None of these event days show any increase in CO, NO, or BC so combustion sources can be deemed negligible. Komenda and Koppmann [2002] report maximum standard emission rates of several monoterpenes by Scots Pine (*Pinus sylvestris*) in April that are ten times higher than those measured in July at a site in central Germany. This is consistent with the April type A maximum observed in this study. Janson [1993] attributes similar seasonal observations of emissions to periods of active needle growth and biosynthesis of monoterpenes. Monoterpene and sesquiterpene oxidation products have been used to explain nucleation events previously [Koch *et al.*, 2000; Bonn and Moortgat, 2003]. Biogenic VOC concentration data are not currently available at TF for these time periods, but future measurements will aid greatly in identifying formation pathways for these events.

[30] A significant fraction of type A events were observed during December–February (38% of the total number observed) when surface temperatures are lower and biological activity is thought to be minimized. However, longer atmospheric hydrocarbon lifetimes due to decreased oxidant concentrations could explain higher than expected winter measurements of monoterpenes [Hakola *et al.*, 2003]. Airborne measurements, mainly in the free troposphere, during the winter/spring over the central Canadian sub-Arctic and Arctic showed very low  $\text{SO}_2$  concentrations (5–60 ppt) and little evidence for new particle formation [Weber *et al.*, 2003b], indicating that the particles observed during PN events at TF likely originated closer to the sampling site than central Canada.

[31] Type B, C, and D events have a very different chemistry given very unique source winds compared to type A events. Growth of  $\text{SO}_4^{2-}$  aerosol is likely during type B and D events because of enhanced  $\text{SO}_2$ . Sulfur dioxide has been shown to be transported long distances associated

with low-level jets [Beyrich, 1995] and therefore may have been emitted from sources in urban areas of the midwestern United States and remained unreacted until reaching the northeastern United States. Iodine or volatile organic compound chemistry may also play an important role in the formation of particles during type C events since southeastern wind directions could have both urban and oceanic influences. Particulate iodine has been identified previously in samples of newly formed ultrafine aerosol at a coastal site in Mace Head, Ireland and was attributed to condensable biogenic iodine-containing precursors [Mäkelä et al., 2002]. Methyl iodide and ethyl iodide concentrations of 0.5–3.5 ppb (similar to measurements at Mace Head by Carpenter et al. [2003]) have been measured at several coastal sites within 15 km of TF [Zhou et al., 2005], and measurements of photolabile chloroiodomethane at TF are reported to be lowest under conditions of strong photochemistry (R. K. Varner et al., 2006, Observations of chloroiodomethane from coastal North Atlantic and remote Pacific regions, manuscript in preparation, 2006). Given southeasterly flow and the localized nature of type C events, it is conceivable that iodine released from these species could contribute upon reaction to new particle formation and growth during type C events.

## 6. Conclusions

[32] One hundred and ninety-five PN concentration events have been identified statistically over a 4-year sampling period at a rural site in New Hampshire. According to event duration and the presence or lack of gaseous pollutants, these events have been segregated into five event types, the most frequent of which were long-lasting events associated with low SO<sub>2</sub> (type A) and events associated with primary pollutants (type E). The exact nature of these events is unknown, but small estimated particle diameters likely indicate the recent growth of aerosols to sizes greater than seven nanometers in diameter from previously formed particles. PN events were not coincident with previously documented smoke and aerosol nitrate events, highlighting the unique characteristics of these events. No correlations between seasonal PN concentrations and climatic anomalies in temperature and precipitation could be made. Additionally, PN events could not be linked to precipitation or temperature fluctuations on a day-to-day basis. Size distributions will be necessary to further elucidate the nature of the identified events. Future measurement of organic aerosol concentrations from daily filters and of NH<sub>3</sub> potentially also will add greatly to understanding the potential for new particle formation and growth at this site. In addition, increased understanding of boundary layer dynamics at this site will be necessary to identify the role of convection and upper-level mixing in PN events [Nilsson et al., 2001]. PN events, like those described here, could have far reaching effects on local and regional air quality, scattering light and affecting cloud dynamics.

[33] **Acknowledgments.** We gratefully acknowledge funding from the Office of Oceanic and Atmospheric Research of the National Oceanic and Atmospheric Administration under AIRMAP grants NA03OAR4600122 and NA04OAR4600154. Any opinions, findings, conclusions and/or recommendations expressed in this material are those of the authors and do not necessarily reflect the views of the funding

agency. We would also like to thank Carolyn Jordan, Ruth Varner, and anonymous reviewers for helpful comments. The authors also gratefully acknowledge the NOAA Air Resources Laboratory for the provision of the HYSPLIT transport and dispersion model and READY website (<http://www.arl.noaa.gov/ready.html>) used in this publication.

## References

- Alam, A., J. P. Shi, and R. M. Harrison (2003), Observations of new particle formation in urban air, *J. Geophys. Res.*, *108*(D3), 4093, doi:10.1029/2001JD001417.
- Anfossi, D., D. Oetl, G. Degrazia, and A. Goulart (2005), An analysis of sonic anemometer observations in low wind speed conditions, *Boundary Layer Meteorol.*, *114*, 179–203.
- Beyrich, F. (1995), Mixing height estimation in the convective boundary layer using Sodar data, *Boundary Layer Meteorol.*, *74*, 1–18.
- Birmili, W., and A. Wiedensohler (2000), New particle formation in the continental boundary layer: Meteorological and gas phase parameter influence, *Geophys. Res. Lett.*, *27*, 3325–3328.
- Birmili, W., H. Berresheim, C. Plass-Dulmer, T. Elste, S. Gilge, A. Wiedensohler, and U. Uhrner (2003), The Hohenpeissenberg aerosol formation experiment (HALFEX): A long-term study including size-resolved aerosol, H<sub>2</sub>SO<sub>4</sub>, OH, and monoterpenes measurements, *Atmos. Chem. Phys.*, *3*, 361–376.
- Bond, T. C., T. L. Anderson, and D. Campbell (1999), Calibration and intercomparison on filter-based measurements of visible light absorption by aerosols, *Aerosol Sci. Technol.*, *30*, 582–600.
- Bonn, B., and G. K. Moortgat (2003), Sesquiterpene ozonolysis: Origin of atmospheric new particle formation from biogenic hydrocarbons, *Geophys. Res. Lett.*, *30*(11), 1585, doi:10.1029/2003GL017000.
- Carpenter, L. J., P. S. Liss, and S. A. Penkett (2003), Marine organohalogen in the atmosphere over the Atlantic and Southern oceans, *J. Geophys. Res.*, *108*(D9), 4256, doi:10.1029/2002JD002769.
- Charlson, R. J., S. E. Schwartz, J. M. Hales, R. D. Cess, J. A. J. Coakley, J. E. Hansen, and D. J. Hofmann (1992), Climate forcing by anthropogenic aerosols, *Science*, *255*, 423–430.
- Clarke, A. D., et al. (1999), Nucleation in the equatorial free troposphere: Favorable environments during PEM-Tropics, *J. Geophys. Res.*, *104*, 5735–5744.
- Day, D. E., and W. C. Malm (2001), Aerosol light scattering measurements as a function of relative humidity: A comparison between measurements made at three different sites, *Atmos. Environ.*, *35*, 5169–5176.
- DeBell, L. J., M. Vozzella, R. W. Talbot, and J. E. Dibb (2004a), Asian dust storm events of spring 2001 and associated pollutants observed in New England by the Atmospheric Investigation, Regional, Modeling, Analysis and Prediction (AIRMAP) monitoring network, *J. Geophys. Res.*, *109*, D01304, doi:10.1029/2003JD003733.
- DeBell, L. J., R. W. Talbot, and J. E. Dibb (2004b), A major regional air pollution event in the northeastern United States caused by extensive forest fires in Quebec, Canada, *J. Geophys. Res.*, *109*, D19305, doi:10.1029/2004JD004840.
- Fischer, E., and R. Talbot (2005), Regional NO<sub>3</sub><sup>-</sup> events in the northeastern United States related to seasonal climate anomalies, *Geophys. Res. Lett.*, *32*, L16804, doi:10.1029/2005GL023490.
- Hakola, H., V. Tarvainen, T. Laurila, V. Hiltunen, H. Hellen, and P. Keronen (2003), Seasonal variation of VOC concentrations above a boreal coniferous forest, *Atmos. Environ.*, *37*, 1623–1634.
- Harrison, R. M., J. L. Grenfell, N. Savage, A. Allen, K. C. Clemitshaw, S. Penkett, C. N. Hewitt, and B. Davidson (2000), Observations of new particle production in the atmosphere of a moderately polluted site in eastern England, *J. Geophys. Res.*, *105*, 17,819–17,832.
- Janson, R. (1993), Monoterpene emissions from Scots pine and Norwegian spruce, *J. Geophys. Res.*, *98*, 2839–2850.
- Jeong, C.-H., G. J. Evans, P. K. Hopke, D. Chalupa, and M. J. Utell (2006), Influence of atmospheric dispersion and new particle formation events on ambient particle number concentration in Rochester, United States, and Toronto, Canada, *J. Air Waste Manage. Assoc.*, *56*, 431–443.
- Koch, S., R. Winterhalter, E. Uherek, A. Kolloff, P. Neeb, and G. K. Moortgat (2000), Formation of new particles in the gas-phase ozonolysis of monoterpenes, *Atmos. Environ.*, *34*, 4031–4042.
- Komenda, M., and R. Koppmann (2002), Monoterpene emissions from Scots pine (*Pinus sylvestris*): Field studies of emission rate variabilities, *J. Geophys. Res.*, *107*(D13), 4161, doi:10.1029/2001JD000691.
- Komppula, M., H. Hihavainen, J. Hatakka, and J. Paatero (2003), Observations of new particle formation and size distributions at two different heights and surroundings in a sub-Arctic area in northern Finland, *J. Geophys. Res.*, *108*(D9), 4295, doi:10.1029/2002JD002939.
- Korhonen, P., M. Kulmala, A. Laaksonen, Y. Viisanen, R. McGraw, and J. H. Seinfeld (1999), Ternary nucleation of H<sub>2</sub>SO<sub>4</sub>, NH<sub>3</sub>, and H<sub>2</sub>O in the atmosphere, *J. Geophys. Res.*, *104*, 26,349–26,353.

- Kulmala, M. (2003), How particles nucleate and grow, *Science*, *302*(5647), 1000–1001.
- Lee, D. S., I. Kohler, E. Grobler, F. Rohrer, R. Sausen, L. Gallardoklenner, J. G. J. Olivier, F. J. Dentener, and A. F. Bouwman (1997), Estimations of global NO<sub>x</sub> emissions and their uncertainties, *Atmos. Environ.*, *31*, 1735–1749.
- Lowenthal, D. H., B. Zielinska, J. C. Chow, J. G. Watson, M. Gautam, D. H. Ferguson, G. R. Neuroth, and K. D. Stevens (1994), Characterization of heavy-duty diesel vehicle emissions, *Atmos. Environ.*, *28*, 731–743.
- Mäkelä, J. M., et al. (1997), Observations of ultrafine aerosol particle formation and growth in the boreal forest, *Geophys. Res. Lett.*, *24*, 1219–1222.
- Mäkelä, J. M., T. Hoffmann, C. Holzke, M. Vakeva, T. Suni, T. Mattila, P. P. Aalto, U. Tapper, E. I. Kauppinen, and C. D. O'Dowd (2002), Biogenic iodine emissions and identification of end-products in coastal ultrafine particles during nucleation events, *J. Geophys. Res.*, *107*(D19), 8110, doi:10.1029/2001JD000580.
- Mao, H., and R. W. Talbot (2004), O<sub>3</sub> and CO in New England: Temporal variations and relationships, *J. Geophys. Res.*, *109*, D21304, doi:10.1029/2004JD004913.
- Marquez, C., T. Castro, A. Muhlia, M. Moya, A. Martinez-Arroyo, and A. Baez (2005), Measurement of aerosol particles, gases and flux radiation in the Pico de Orizaba National Park, and its relationship to air pollution transport, *Atmos. Environ.*, *39*, 3877–3890.
- Mozurkewich, M., T.-W. Chan, Y.-A. Aklilu, and B. Verheggen (2004), Aerosol particle size distributions in the lower Fraser Valley: Evidence for particle nucleation and growth, *Atmos. Chem. Phys.*, *4*, 1047–1062.
- Nilsson, E. D., U. Rannik, M. Kulmala, G. Buzorius, and C. D. O'Dowd (2001), Effects of continental boundary layer evolution, convection, turbulence and entrainment, on aerosol formation, *Tellus, Ser. B*, *53*, 441–461.
- O'Dowd, C. D., et al. (2002), Coastal new particle formation: Environmental conditions and aerosol physicochemical characteristics during nucleation bursts, *J. Geophys. Res.*, *107*(D19), 8107, doi:10.1029/2000JD000206.
- Parungo, F., C. Nagamoto, M. Zhou, A. D. A. Hansen, and J. Harris (1994), Aeolian transport of aerosol black carbon from China to the ocean, *Atmos. Environ.*, *28*, 2715–2725.
- Shetter, R. E., et al. (2003), Photolysis frequency of NO<sub>2</sub>: Measurement and modeling during the International Photolysis Frequency Measurement and Modeling Intercomparison (IPMMI), *J. Geophys. Res.*, *108*(D16), 8544, doi:10.1029/2002JD002932.
- Stanier, C. O., A. Y. Khlystov, and S. N. Pandis (2004), Nucleation events during the Pittsburgh air quality study: Description and relation to key meteorological, gas phase, and aerosol parameters, *Aerosol Sci. Tech.*, *38*, 253–264.
- Stolzenburg, M. R., P. H. McMurry, H. Sakurai, J. N. Smith, R. L. Mauldin, F. L. Eisele, and C. F. Clement (2005), Growth rates of freshly nucleated atmospheric particles in Atlanta, *J. Geophys. Res.*, *110*, D22S05, doi:10.1029/2005JD005935.
- Vehkamäki, H., et al. (2004), Atmospheric particle formation events at Varrio measurement station in Finnish Lapland 1998–2002, *Atmos. Chem. Phys.*, *4*, 2015–2023.
- Verheggen, B., and M. Mozurkewich (2002), Determination of nucleation and growth rates from observation of a SO<sub>2</sub> induced atmospheric nucleation event, *J. Geophys. Res.*, *107*(D11), 4123, doi:10.1029/2001JD000683.
- Vose, R. S. (2005), Reference station networks for monitoring climatic change in the conterminous United States, *J. Clim.*, *18*, 5390–5395.
- Weber, R. J., P. H. McMurry, F. L. Eisele, and D. J. Tanner (1995), Measurement of expected nucleation precursor species and 3–500-nm diameter particles at Mauna Loa observatory, Hawaii, *J. Atmos. Sci.*, *58*, 2242–2257.
- Weber, R. J., et al. (2003a), New particle formation in anthropogenic plumes advecting from Asia observed during TRACE-P, *J. Geophys. Res.*, *108*(D21), 8814, doi:10.1029/2002JD003112.
- Weber, R. J., et al. (2003b), Investigations into free tropospheric new particle formation in the central Canadian arctic during the winter/spring transition as part of TOPSE, *J. Geophys. Res.*, *108*(D4), 8357, doi:10.1029/2002JD002239.
- Whitby, K. T., and G. M. Sverdrup (1980), California aerosols: Their physical and chemical characteristics, *Adv. Environ. Sci. Technol.*, *8*, 477–525.
- Zhou, Y., R. K. Varner, R. S. Russo, O. W. Wingenter, K. B. Haase, R. Talbot, and B. C. Sive (2005), Coastal water source of short-lived halocarbons in New England, *J. Geophys. Res.*, *110*, D21302, doi:10.1029/2004JD005603.

---

R. J. Griffin, R. W. Talbot, and L. D. Ziemba, Institute for the Study of Earth, Oceans, and Space, Climate Change Research Center, University of New Hampshire, Morse Hall, 39 College Road, Durham, NH 03824, USA. (rob.griffin@unh.edu)